

# Extraction of the proton mass radius from the vector meson photoproductions near thresholds

Rong Wang,<sup>1,2,\*</sup> Wei Kou,<sup>1,2,†</sup> Ya-Ping Xie,<sup>1,2,‡</sup> and Xurong Chen<sup>1,2,3,§</sup>

<sup>1</sup>*Institute of Modern Physics, Chinese Academy of Sciences, Lanzhou 730000, China*

<sup>2</sup>*University of Chinese Academy of Sciences, Beijing 100049, China*

<sup>3</sup>*Guangdong Provincial Key Laboratory of Nuclear Science, Institute of Quantum Matter, South China Normal University, Guangzhou 510006, China*

(Dated: February 28, 2025)

We present an analysis of the proton mass radius by studying the  $t$ -dependence of the differential cross sections of the vector meson photoproductions near thresholds. At low energy, the photoproduction of quarkonium off the proton is connected to the scalar gravitational form factor of the proton, which is sensitive to the proton mass distribution from the trace anomaly. Under an assumption of the scalar form factor of dipole form, the proton mass radius is extracted via the near-threshold photoproduction data of  $J/\psi$ ,  $\phi$  and  $\omega$  vector mesons. The average value of the proton mass radius is estimated to be  $\sqrt{\langle R_m^2 \rangle} = 0.67 \pm 0.03$  fm, with the dipole cutoff  $m_s = 1.01 \pm 0.04$  GeV.

In modern physics, the proton is viewed as a confined system of quarks and gluons with energy and pressure inside governed by the strong interaction. The underlying theory of strong interaction is quantum chromodynamics (QCD). Understanding the color confinement and the mass generation of the proton in QCD theory is one of the deepest questions in particle and nuclear physics. As a composite particle, various distributions are often used to describe the proton, such as the charge distribution, the current distribution and the mass distribution. Up to date, the charge radius and the magnetic radius of the proton are precisely measured, with  $R_C = 0.8409 \pm 0.0004$  fm and  $R_{\text{mag.}} = 0.851 \pm 0.026$  fm [1]. However in experiment the mass radius of the proton is still unknown.

In theory, the basic mechanical properties of the proton are well encoded in the energy-momentum tensor  $T_{\mu\nu}$  (EMT) [2–4]. By investigating the trace of EMT, Ji suggests a decomposition of the proton mass including the quantum anomalous energy of QCD [5–8]. This mass decomposition is further studied with the lattice QCD (LQCD) calculation [9] and the preliminary analysis of  $J/\psi$  photoproduction data [10, 11]. Recently the renormalization of EMT and the scheme-dependence of proton mass decompositions are carefully studied and discussed [12, 13]. Though there is still a long way to have a final decomposition of the proton mass, the origin of the proton mass can be understood in QCD theory.

The proton matrix element of EMT contains three gravitational form factors (GFFs) ( $A(t)$ ,  $B(t)$ ,  $D(t)$ )

[3, 4, 14–17], which is written as,

$$\begin{aligned} \langle p' | T_{\mu\nu} | p \rangle = & \bar{u}' \left[ A(t) \frac{\gamma_{\{\mu} P_{\nu\}}}{2} + B(t) \frac{i P_{\{\mu} \sigma_{\nu\}} \Delta^\rho}{4m} \right. \\ & \left. + D(t) \frac{\Delta_\mu \Delta_\nu - g_{\mu\nu} \Delta^2}{4m} + m \bar{c}(t) g_{\mu\nu} \right] u e^{i(p'-p)x}, \end{aligned} \quad (1)$$

where the kinematic variables are  $P = \frac{1}{2}(p' + p)$ ,  $\Delta = p' - p$ ,  $t = \Delta^2$ , and the covariant normalization is expressed as  $\langle p' | p \rangle = 2p^0 (2\pi)^3 \delta^{(3)}(\mathbf{p}' - \mathbf{p})$ . Using the Gordon identity  $2m \bar{u}' \gamma^\alpha u = \bar{u}' (2P^\alpha + i\sigma^{\alpha\kappa} \Delta_\kappa) u$  an alternative decomposition is given by [17],

$$\begin{aligned} \langle p' | T_{\mu\nu} | p \rangle = & \bar{u}' \left[ A(t) \frac{P_\mu P_\nu}{m} + J(t) \frac{i P_{\{\mu} \sigma_{\nu\}} \Delta^\rho}{2m} \right. \\ & \left. + D(t) \frac{\Delta_\mu \Delta_\nu - g_{\mu\nu} \Delta^2}{4m} + m \bar{c}(t) g_{\mu\nu} \right] u e^{i(p'-p)x}. \end{aligned} \quad (2)$$

The Fourier transforms of the GFFs  $A(t)$ ,  $J(t)$  and  $D(t)$  provide the mass distribution [3, 4, 6, 7, 17], the angular momentum distribution [4, 14, 15, 18] and the pressure distribution [16, 17, 19] inside the proton respectively.  $A(t)$ ,  $B(t)$  and  $D(t)$  are all renormalization scale invariant, since here the GFFs are defined as the sum of quark and gluon contributions. As a consequence of momentum conservation, the constraint  $A(0) = 1$  is given [14, 15, 17]. Recently the form factor of  $T_{00}$  is suggested to be the mass form factor [5, 20].

On the theoretical side, there are many progresses which have been made on the GFFs, such as LQCD [21], holographic QCD [22], light-cone QCD [23], MIT bag model [24], NJL model [25], chiral perturbation theory [26–28], instanton model [29], QCD sum rule [30] and the dispersion relation [31]. The form factors of the proton are usually described with the dipole form, which corresponds to an exponential distribution of the concerned quantity of the proton. For the dipole form parametrization  $A(t) = A(0) / \left(1 - \frac{t}{m_A^2}\right)^2$ , LQCD calculation gives  $m_A = 1.13 \pm 0.06$  GeV [21] and the soft-wall model of

\* rwang@impcas.ac.cn

† kouwei@impcas.ac.cn

‡ xieyaping@impcas.ac.cn

§ xchen@impcas.ac.cn

holographic QCD gives  $m_A = 1.124$  GeV [22]. The dipole gravitational form factor also meets the asymptotic behavior of the GFFs at large momentum based on the perturbative QCD [32] and the power counting analysis [33–35].

To access the mechanical properties of the proton, the electromagnetic interaction can be used. In principle, the GFFs of the proton can be extracted from the generalized parton distributions (GPD) with the full  $t$ -dependence and  $\xi$ -dependence [17, 19]. Using the dispersion relation, the GFF  $D(t)$  was indirectly extracted from the deeply virtual Compton scattering (DVCS) data in a recent analysis [19]. The peak repulsive pressure about  $10^{35}$  pascals is deduced from the analysis of  $D(t)$ . Moreover, the repulsive pressure and the confining pressure are balanced around  $r = 0.6$  fm [19]. For the pion, the mass radius has been reported to be  $0.32 \sim 0.39$  fm by S. Kumano et al, via the measurement of the generalized distribution amplitude (GPA) of the pion [36]. The obtained mass radius of the pion is significantly smaller than the charge radius of the pion, and it is consistent with the NJL model [25].

It is interesting to search for new experimental methods beside the measurements of GPD and GPA to acquire the GFFs of the proton. In the framework of holographic QCD, the diffractive photoproductions of heavy quarkonia on the proton are connected to the GFFs of the proton [22, 37–39]. The near-threshold  $J/\psi$  and  $\Upsilon$  productions in e-p scattering and p-A ultraperipheral collision are suggested to study the proton mass problem [38, 39]. Based on the holographic QCD model, a recent calculation shows that the elastic proton-proton scattering can be used to test the GFFs [40]. The more reliable way is to employ the van der Waals interaction between the color dipole and the proton at low energy suggested by D. Kharzeev [20, 41], which is a famous vector-meson-dominance (VMD) model. The scalar gravitational form factor of the trace of the EMT is measured via the interaction between the dipole and the proton. Following Kharzeev's work and assuming a dipole form GFF, we performed an analysis of the proton mass radius from the differential cross section data of the near-threshold vector meson photoproductions, including the data of  $J/\psi$ ,  $\phi$  and  $\omega$ .

In the non-relativistic limit, the mass distribution can be defined using the scalar gravitational form factor instead of the form factor of  $T_{00}$  [20], which is written as,

$$\langle R_m^2 \rangle = \frac{6}{M} \left. \frac{dG(t)}{dt} \right|_{t=0}, \quad (3)$$

with  $G(0) = M$ . The scalar gravitational form factor is defined as the matrix element of the trace of the EMT, which is written as [5, 20],

$$G(t) = MA(t) - B(t) \frac{t}{4M} + D(t) \frac{3t}{M}. \quad (4)$$

The gravitational form factors are usually parameterized

as the dipole form. Therefore we have,

$$G(t) = \frac{M}{(1 - t/m_s^2)^2}, \quad (5)$$

in which  $m_s$  is an unknown parameter to be determined in experiment. According to the definition, the mass radius is connected to the dipole parameter  $m_s$  as,

$$\langle R_m^2 \rangle = \frac{12}{m_s^2}. \quad (6)$$

The near-threshold cross section of quarkonium photoproduction is directly related to the matrix element of the scalar gluon operator, hence the scalar gravitational form factor [20, 41]. The differential cross section of the photoproduction of the quarkonium can be described with the GFFs, which is written as [20, 22, 37, 42],

$$\frac{d\sigma}{dt} \propto G^2(t). \quad (7)$$

By studying the differential cross section of the vector meson photoproduction off the proton, we can extract the parameter  $m_s$  of the scalar form factor. Then we acquire the radius information by using Eq. (6).

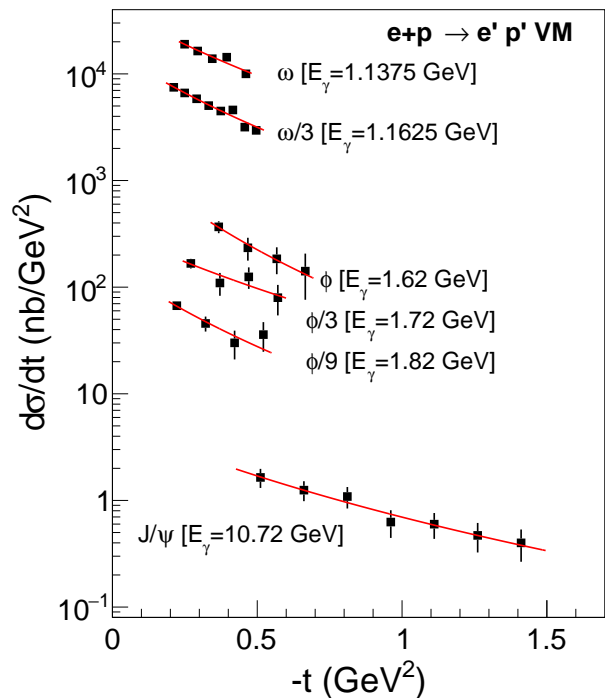


FIG. 1. The differential cross sections of the photoproductions of  $J/\psi$  [10],  $\phi$  [43] and  $\omega$  [44] vector mesons near the thresholds. The energies of the incident photons are labeled in the figure for the experimental data. Some of the cross sections are scaled with the factors, which are also indicated in the figure.

Fig. 1 shows the differential cross sections of the vector meson photoproductions as a function of  $-t$ .

The differential cross sections are fitted with the scalar gravitational form factor of the dipole parametrization (see the curves in Fig. 1). The only heavy quarkonium photoproduction data near the threshold is from GlueX [10]. We determined the dipole parameter to be  $m_s = 1.23 \pm 0.19$  GeV, and the proton mass radius to be  $\sqrt{\langle R_m^2 \rangle} = 0.55 \pm 0.09$  fm, from the fit to the  $J/\psi$  data. In experiment, there are already some data on the near-threshold photoproductions of light quarkonia. We take the differential cross sections of near-threshold  $\phi$  photoproduction at different photon energies by LEPS Collaboration [43]. The extracted dipole parameter and the proton mass radii are listed in Table I, from the fit to the  $\phi$  data. The average mass radius of the three extracted values is obtained to be  $\sqrt{\langle R_m^2 \rangle} = 0.67 \pm 0.10$  fm. We take the differential cross sections of near-threshold  $\omega$  photoproduction at different photon energies by SAPHIR at ELSA [44]. The extracted dipole parameter and the proton mass radii are listed in Table II, from the fit to the  $\omega$  data. The average mass radius of the two extracted values is obtained to be  $\sqrt{\langle R_m^2 \rangle} = 0.68 \pm 0.03$  fm.

Fig. 2 shows the extracted proton mass radius as a function of the mass of the vector meson, which comes from the color dipole interacting with the proton target. The extracted values are consistent with each other within the statistical uncertainties. The combined analysis of the data of the three vector mesons gives the average proton mass radius to be  $\sqrt{\langle R_m^2 \rangle} = 0.67 \pm 0.03$  fm, with the average dipole parameter to be  $m_s = 1.01 \pm 0.04$  GeV.

TABLE I. The extracted values of the dipole parameter and the proton mass radii from the differential cross sections of  $\phi$  photoproduction near threshold at different photon energies.

$E_\gamma$ (GeV)	1.62	1.72	1.82
$m_s$ (GeV)	$0.82 \pm 0.24$	$1.17 \pm 0.30$	$0.96 \pm 0.20$
$\sqrt{\langle R_m^2 \rangle}$ (fm)	$0.83 \pm 0.25$	$0.58 \pm 0.15$	$0.71 \pm 0.15$

TABLE II. The extracted values of the dipole parameter and the proton mass radii from the differential cross sections of  $\omega$  photoproduction near threshold at different photon energies.

$E_\gamma$ (GeV)	1.135	1.165
$m_s$ (GeV)	$1.06 \pm 0.06$	$0.99 \pm 0.04$
$\sqrt{\langle R_m^2 \rangle}$ (fm)	$0.65 \pm 0.04$	$0.69 \pm 0.03$

Now there is a heating discussion on building a low energy Electron-ion collider in China (EicC), by upgrading the High-Intensity heavy-ion Accelerator Facility (HIAF) with a polarized electron accelerator [45–47]. The center-of-mass energy of e-p collision is around 20 GeV, which provides a good opportunity to study the near-threshold  $\Upsilon$  photoproduction by exploiting the virtual photon flux.

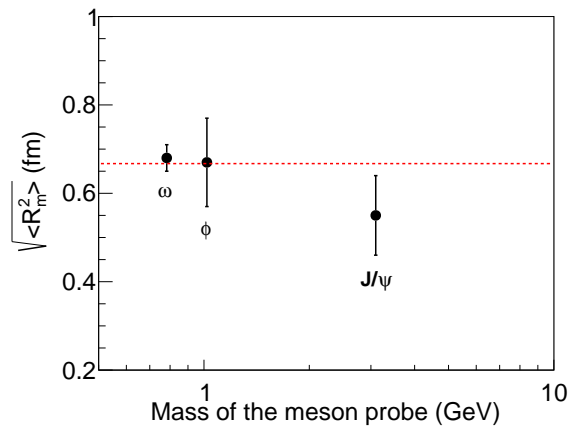


FIG. 2. The proton mass radii from different meson production channels. The dash line shows the average value from the least-square fit.

The  $\Upsilon$  photoproduction events at EicC are all near the threshold energy and of the low  $Q^2$ . The electroproduction cross section of  $\Upsilon$  at EicC energy has already been estimated using the pomeron exchange model and the two-gluon exchange model, which is at the magnitude of 100 fb at 20 GeV [48]. According to a recent calculation [39], the near-threshold heavy quarkonia electroproductions at large  $Q^2$  provide the important information about the origin of proton mass and the mass distribution, which can be realized with the Electron-Ion Collider in US (EIC) [49]. The  $\Upsilon$  production experiment at EicC and EIC will be a strict test of the GFFs and the VMD model in the bottom quark sector. This will improve our understanding on the proton mass distribution. Excitingly the large intensity facility of the SoLID program at JLab can provide a precise measurement of the proton mass distribution with the near-threshold  $J/\psi$  electroproduction data. These future near-threshold photoproductions of heavy quarkonia surely will play an important role in revealing the mass distribution and the mass radius of the proton.

The photon-induced vector meson productions off the proton can be described with the scalar GFF of the dipole form. By using this model, we have extracted the proton mass radius to be  $\sqrt{\langle R_m^2 \rangle} = 0.67 \pm 0.03$  fm from a combined analysis of the data of  $J/\psi$ ,  $\phi$  and  $\omega$ , which is obviously smaller than the charge radius or the magnetic radius of the proton. This is very similar to the case for the pion [36]. Our obtained radius is close to the LQCD calculation ( $0.62 \pm 0.03$  fm with  $m_A = 1.13 \pm 0.06$  GeV) [21] and the holographic QCD calculation (0.62 fm with  $m_A = 1.124$  GeV) [22]. We find that the mass radius is at somewhere of the proton pressure  $r^2 p(r)$  crossing zero [19]. The light vector meson data show the larger mass radius than that from the  $J/\psi$  data. This is maybe due to the size effect or the mass effect of the color-dipole, or the validity of applying the VMD model for the near-threshold light vector meson productions. The obviously

smaller mass radius indicates that the energy distribution is significantly different from the charge distribution. Since the energy distribution is mainly coupled to the gluons and the charge distribution is coupled to the quarks, Kharzeev guesses that the smaller mass radius comes from the smaller gluon radius, or from the interplay of scale anomaly and spontaneously broken chiral symmetry [20].

## ACKNOWLEDGMENTS

We thank Nu XU for the fruitful discussions. This work is supported by the Strategic Priority Research Program of Chinese Academy of Sciences under the Grant NO. XDB34030301 and the National Natural Science Foundation of China under the Grant NO. 12005266.

- 
- [1] P. A. Zyla *et al.* (Particle Data Group), PTEP **2020**, 083C01 (2020).
- [2] I. Y. Kobzarev and L. B. Okun, Zh. Eksp. Teor. Fiz. **43**, 1904 (1962).
- [3] H. Pagels, Phys. Rev. **144**, 1250 (1966).
- [4] X.-D. Ji, Phys. Rev. D **55**, 7114 (1997), arXiv:hep-ph/9609381.
- [5] X. Ji and Y. Liu, (2021), arXiv:2101.04483 [hep-ph].
- [6] X.-D. Ji, Phys. Rev. Lett. **74**, 1071 (1995), arXiv:hep-ph/9410274.
- [7] X.-D. Ji, Phys. Rev. D **52**, 271 (1995), arXiv:hep-ph/9502213.
- [8] C. Lorcé, Eur. Phys. J. C **78**, 120 (2018), arXiv:1706.05853 [hep-ph].
- [9] Y.-B. Yang, J. Liang, Y.-J. Bi, Y. Chen, T. Draper, K.-F. Liu, and Z. Liu, Phys. Rev. Lett. **121**, 212001 (2018), arXiv:1808.08677 [hep-lat].
- [10] A. Ali *et al.* (GlueX), Phys. Rev. Lett. **123**, 072001 (2019), arXiv:1905.10811 [nucl-ex].
- [11] R. Wang, J. Evslin, and X. Chen, Eur. Phys. J. C **80**, 507 (2020), arXiv:1912.12040 [hep-ph].
- [12] A. Metz, B. Pasquini, and S. Rodini, Phys. Rev. D **102**, 114042 (2021), arXiv:2006.11171 [hep-ph].
- [13] S. Rodini, A. Metz, and B. Pasquini, JHEP **09**, 067 (2020), arXiv:2004.03704 [hep-ph].
- [14] X.-D. Ji, Phys. Rev. D **58**, 056003 (1998), arXiv:hep-ph/9710290.
- [15] O. V. Teryaev, Front. Phys. (Beijing) **11**, 111207 (2016).
- [16] M. V. Polyakov, Phys. Lett. B **555**, 57 (2003), arXiv:hep-ph/0210165.
- [17] M. V. Polyakov and P. Schweitzer, Int. J. Mod. Phys. A **33**, 1830025 (2018), arXiv:1805.06596 [hep-ph].
- [18] X.-D. Ji, Phys. Rev. Lett. **78**, 610 (1997), arXiv:hep-ph/9603249.
- [19] V. D. Burkert, L. Elouadrhiri, and F. X. Girod, Nature **557**, 396 (2018).
- [20] D. E. Kharzeev, (2021), arXiv:2102.00110 [hep-ph].
- [21] P. E. Shanahan and W. Detmold, Phys. Rev. D **99**, 014511 (2019), arXiv:1810.04626 [hep-lat].
- [22] K. A. Mamo and I. Zahed, Phys. Rev. D **101**, 086003 (2020), arXiv:1910.04707 [hep-ph].
- [23] K. Azizi and U. Özdem, Eur. Phys. J. C **80**, 104 (2020), arXiv:1908.06143 [hep-ph].
- [24] M. J. Neubelt, A. Sampino, J. Hudson, K. Tezgin, and P. Schweitzer, Phys. Rev. D **101**, 034013 (2020), arXiv:1911.08906 [hep-ph].
- [25] A. Freese and I. C. Cloët, Phys. Rev. C **100**, 015201 (2019), arXiv:1903.09222 [nucl-th].
- [26] J.-W. Chen and X.-d. Ji, Phys. Rev. Lett. **88**, 052003 (2002), arXiv:hep-ph/0111048.
- [27] A. V. Belitsky and X. Ji, Phys. Lett. B **538**, 289 (2002), arXiv:hep-ph/0203276.
- [28] M. Diehl, A. Manashov, and A. Schafer, Eur. Phys. J. A **31**, 335 (2007), arXiv:hep-ph/0611101.
- [29] M. V. Polyakov and H.-D. Son, JHEP **09**, 156 (2018), arXiv:1808.00155 [hep-ph].
- [30] I. V. Anikin, Phys. Rev. D **99**, 094026 (2019), arXiv:1902.00094 [hep-ph].
- [31] B. Pasquini, M. V. Polyakov, and M. Vanderhaeghen, Phys. Lett. B **739**, 133 (2014), arXiv:1407.5960 [hep-ph].
- [32] X.-B. Tong, J.-P. Ma, and F. Yuan, (2021), arXiv:2101.02395 [hep-ph].
- [33] S. J. Brodsky and G. R. Farrar, Phys. Rev. Lett. **31**, 1153 (1973).
- [34] V. A. Matveev, R. M. Muradian, and A. N. Tavkhelidze, Lett. Nuovo Cim. **7**, 719 (1973).
- [35] X.-d. Ji, J.-P. Ma, and F. Yuan, Phys. Rev. Lett. **90**, 241601 (2003), arXiv:hep-ph/0301141.
- [36] S. Kumano, Q.-T. Song, and O. V. Teryaev, Phys. Rev. D **97**, 014020 (2018), arXiv:1711.08088 [hep-ph].
- [37] Y. Hatta and D.-L. Yang, Phys. Rev. D **98**, 074003 (2018), arXiv:1808.02163 [hep-ph].
- [38] Y. Hatta, A. Rajan, and D.-L. Yang, Phys. Rev. D **100**, 014032 (2019), arXiv:1906.00894 [hep-ph].
- [39] R. Boussarie and Y. Hatta, Phys. Rev. D **101**, 114004 (2020), arXiv:2004.12715 [hep-ph].
- [40] W. Xie, A. Watanabe, and M. Huang, JHEP **10**, 053 (2019), arXiv:1901.09564 [hep-ph].
- [41] H. Fujii and D. Kharzeev, Phys. Rev. D **60**, 114039 (1999), arXiv:hep-ph/9903495.
- [42] L. Frankfurt and M. Strikman, Phys. Rev. D **66**, 031502 (2002), arXiv:hep-ph/0205223.
- [43] T. Mibe *et al.* (LEPS), Phys. Rev. Lett. **95**, 182001 (2005), arXiv:nucl-ex/0506015.
- [44] J. Barth *et al.*, Eur. Phys. J. A **18**, 117 (2003).
- [45] X. Chen, *Proceedings, 26th International Workshop on Deep Inelastic Scattering and Related Subjects (DIS 2018): Port Island, Kobe, Japan, April 16-20, 2018*, PoS **DIS2018**, 170 (2018), arXiv:1809.00448 [nucl-ex].
- [46] X. Chen, F.-K. Guo, C. D. Roberts, and R. Wang, Few Body Syst. **61**, 43 (2020), arXiv:2008.00102 [hep-ph].
- [47] D. P. Anderle *et al.*, (2021), arXiv:2102.09222 [nucl-ex].
- [48] Y. Xu, Y. Xie, R. Wang, and X. Chen, Eur. Phys. J. C **80**, 283 (2020), arXiv:2002.05340 [hep-ph].
- [49] A. Accardi *et al.*, Eur. Phys. J. A **52**, 268 (2016), arXiv:1212.1701 [nucl-ex].